SWI-INFORMED DIFFUSION TENSOR TRACTOGRAPHY

M. Kleinnijenhuis[1,2], M. Barth[1,3], D. C. Alexander[4], A-M. van Cappellen van Walsum[2,5], and D. G. Norris[1,3]
[1]Radboud University Nijmegen, Donders Institute for Brain, Cognition and Behaviour, Nijmegen, Netherlands, [2]Department of Anatomy, University Medical Centre St. Radboud, Nijmegen, Netherlands, [3]Erwin L. Hahn Institute for Magnetic Resonance Imaging, Essen, Germany, [4]Centre for Medical Image Computing, Department of Computer Science, University College London, London, United Kingdom, [5]MIRA Institute for Biomedical Technology and Technical Medicine, University of Twente, Enschede, Netherlands

Introduction

In diffusion tensor tractography (DTT), white matter structure is inferred *in vivo* by reconstructing fiber tracts from diffusion weighted images (DWI). Recently [1], white matter structure has also been shown at 7T using susceptibility weighted imaging (SWI) [2]. Most notably, SWI shows excellent contrast between the highly myelinated optic radiation (OR) and the surrounding white matter [3]. Because DTT attempts to reconstruct tracts from voxels orders of magnitude larger than the underlying substrate, it suffers from partial volume effects in voxels that contain multiple or incoherently oriented tracts, resulting in false positive and false negative tracts. Tractography might therefore benefit from the combination of the diffusion tensor with the white matter contrasts in SWI which can be obtained at a much higher resolution. We have adapted a DTT algorithm to include the structure tensor [4] of the SWI magnitude in order to improve tractography in locations where DWI and SWI provide complementary information.

Methods

DWI (3T; 32-ch coil; twice-refocused spin echo EPI; 61+7 gradient directions; b=1000 s/mm^2; TR=8300 ms; TE=95 ms; matrix size=110x110; FOV=220x220 mm; slice thickness=2.0 mm; number of slices=64) and SWI (7T; 8-ch coil; sagittal orientation; TR=36 ms; TE=25 ms; flip angle=15°; matrix size=448x336; FOV=224x168 mm; slice thickness=0.5 mm; number of slices=208; BW=120 Hz/px; acquisition time=20 min) were recorded from a healthy volunteer. The DWI mean b0 image and SWI were bias field corrected and then coregistered with FSL using the normalized mutual information algorithm and weighting volumes. The diffusion tensor and structure tensor fields were reconstructed from the DWI and SWI volumes, respectively. The structure tensor was calculated as the partial derivatives [d_{xx},d_{xy},d_{xz}; d_{yx},d_{yy},d_{yz}; d_{zx},d_{zy},d_{zz}] of the SWI magnitude and every structure tensor component was smoothed (FWHM = 2.5 mm). Tractography was performed using Camino (PICo; 5000 iterations; curvature threshold = 80º; FA threshold = 0.10; step size = 0.50 mm). The structure tensor information was incorporated by requiring that the tracking direction be in the plane orthogonal to the first eigenvector of the structure tensor (ST ϵ_1). This plane is assumed to be aligned to the direction of the tract that causes the intensity variation. The tracking direction within this plane is determined as the projection of the diffusion tensor onto the plane. To avoid adapted tracking directions where the structure tensor was non-informative, it was used only if the first eigenvalue of the structure tensor (ST λ_1) > 100. For evaluating the performance, seeds were placed in the OR posterior to the point where it merged with the splenium of the corpus callosum (SCC). Waypoints were created anterior to the split in both the OR and SCC. Fractions of streamlines crossing these waypoints were extracted for both DTT and SWI-informed DTT.

Results and Discussion

Although the main tracts were similar for both DTT and SWI-informed DTT, the algorithms often showed very different branching patterns and more subtle differences in the course of the tracts. Examples are provided in Fig 1&2. In Fig 1 a putatively more accurate tracking of the OR using SWI-informed DTT compared to DTT is shown after seeding in the posterior OR. The seed at the merging of the OR and the SCC resulted in markedly different results for DTT and SWI-informed DTT (Fig 2). Frontal branches emerged for SWI-informed DTT, but not for DTT. A presumably non-veridical split is seen in the SCC for SWI-informed DTT (black arrow), where the structure tensor seems to cause a bias towards the borders of the tract. Fractions of streamlines entering OR/SCC were 0.026 for DTT vs. 0.336 for SWI-informed DTT.

Conclusions

A modification of a method was proposed to overcome some limitations of diffusion tensor tractography. It was shown that the contrast within the white matter in susceptibility weighted images can provide additional information for tractography algorithms, leading to increased sensitivity at specific locations. To have an unambiguous validation of the findings of SWI-informed DTT, an *ex vivo* validation of white matter connectivity has to be performed. We have shown that SWI-informed DTT reveals white matter fiber tracts that were not found using standard DTT.

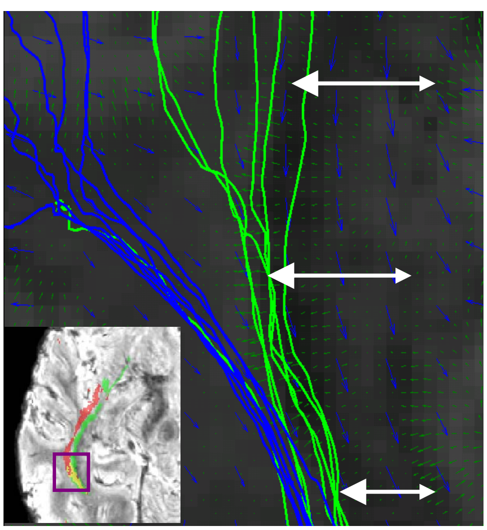

Figure 1. SWI-informed DTT follows the lateral border of the OR (white arrows). Note the orthogonal orientations of the ST and DT. Inset shows connectivity map (green tracts=SWI-informed DTT; green arrows= ST ϵ_1; blue tracts=DTT; blue arrows= DT ϵ_1; yellow area=common tracts).

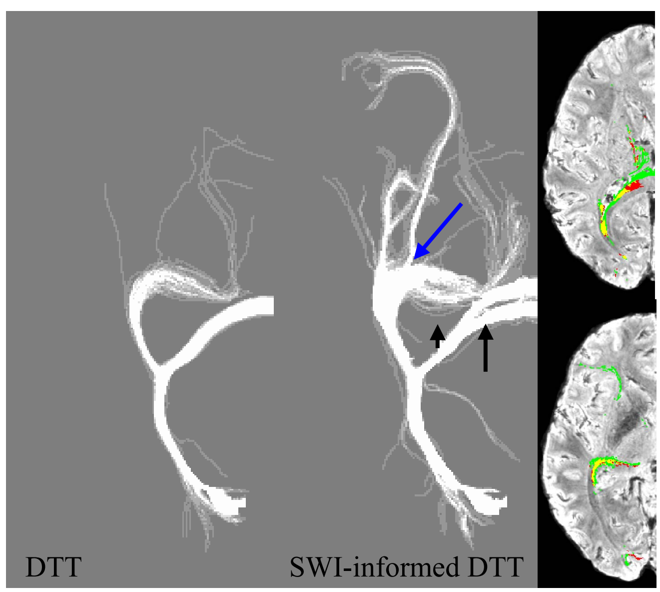

Figure 2. Different branching (blue arrow) and tract paths (black arrows) for DTT (left) and SWI-informed DTT (middle) in axial maximum intensity projection. Left panel shows axial slices with connectivity maps at the level of the merging of the OR and SCC and Meyer's loop (red=DTT; green=SWI-informed DTT; yellow=common).

[1] Li et al, Neuroimage 2006

[2] Haacke and Reichenbach, MRM 2004

[3] Mori et al, Invest Radiol 2009

[4] O'Donnell et al, MICCAI 2004